SYNCHRONIZABILITY OF NETWORKS WITH STRONGLY DELAYED LINKS: A UNIVERSAL CLASSIFICATION

V. FLUNKERT, S. YANCHUK, T. DAHMS, AND E. SCHÖLL

ABSTRACT. We show that for large coupling delays the synchronizability of delay-coupled networks of identical units relates in a simple way to the spectral properties of the network topology. The master stability function used to determine stability of synchronous solutions has a universal structure in the limit of large delay: it is rotationally symmetric around the origin and increases monotonically with the radius in the complex plane. We give details of the proof of this structure and discuss the resulting universal classification of networks with respect to their synchronization properties. We illustrate this classification by means of several prototype network topologies.

CONTENTS

1. INTRODUCTION

Synchronization phenomena of coupled nonlinear oscillators are omnipresent and play an important role in physical, chemical and biological systems [1, 2, 3, 4]. Understanding the synchronization mechanisms is crucial for many practical applications.

One of the most intriguing effects occurring in coupled nonlinear systems is the synchronization of chaotic dynamics [5]. The notions of chaos and synchronization apparently contradict each other. A system is chaotic if small perturbations of the system's initial condition are amplified resulting in an unpredictable dynamical behavior. Stable synchronization of two systems on the other hand occurs when deviations between the system states decay with time (negative transversal Lyapunov exponent).

The contradiction between these two characteristics is only apparent because the decay and amplification occur in different directions in phase space. Perturbations

within the synchronization manifold (SM), i.e., the manifold on which the states of the two systems are identical, grow due to a positive Lyapunov exponent within this manifold giving rise to the chaotic dynamics. On the other hand, perturbations transversal to the SM, associated with deviations between the two systems, decay due to a negative transverse Lyapunov exponent, thus leading to stable synchronization. Another aspect is the influence of delayed coupling, since time delay renders the phase space infinite-dimensional and may on one hand induce instabilities and bifurcations, or may on the other hand stabilize unstable states [6, 7, 8, 9].

Semiconductor lasers are of particular interest in the study of chaos synchronization. The synchronization properties may lead to potential applications, e.g., to new secure communication schemes [10, 11, 12, 13, 14, 15, 16, 17, 18, 19]. However, it is impossible to synchronize chaos in two delay-coupled systems without self-feedback for large delays because the synchronized solution is always transversely unstable. In coupled lasers this effect leads to spontaneous symmetry breaking, and only generalized synchronization of leader-laggard type occurs [20].

However, chaos synchronization of two delay coupled systems can be stable if each system has self-feedback. For semiconductor lasers this has been realized with a passive relay in form of a semitransparent mirror or an active relay in form of a third laser in between the two lasers [21, 22, 23, 24]. These structures are thus interesting for chaos based communication systems.

For practical applications it is not only necessary that the synchronized solution is (linearly) stable, but it is also important how robust the synchronization is to noise. Here, nonlinear effects may play an important role. In particular, for synchronized chaotic systems bubbling [25, 26] plays a key role in this context. This effect may lead to occasional desynchronization even for arbitrarily small noise amplitudes. Bubbling has been observed for example in optical [27, 28] and electrical [29] systems. This paper reviews and extends our recent letter [30] on synchronization in delay-coupled networks with large delay, providing a universal classification [31].

2. Structure of the master stability function for large delay

To determine the stability of a synchronized state in a network of identical units, a powerful method has been developed [32, 33] called the master stability function (MSF). The MSF for networks with coupling delays has been the subject of recent works [34, 35, 36]. Time delay effects play an important role in realistic networks. For example, the finite propagation time of light between coupled semiconductor lasers [37, 38, 39, 21, 40, 41, 42, 43, 44] significantly influence the dynamics. Similar effects occur in neuronal [45, 46, 47, 48, 49, 50, 51, 52, 53] and biological [54] networks.

In this work we show [30] that the MSF for networks with coupling delays has a very simple structure in the limit of large delays. This allows us to prove a number of general statements about the synchronizability of such networks.

We will first discuss the MSF approach and since we are interested in delay coupled systems, we will do this in the context of networks with delay [34, 35, 36].

3. Stability of synchronized solutions

Consider a system of N identical units connected in a network with a coupling delay τ [35]

$$(3.1) \qquad \frac{d}{dt} x^i(t) = f\left[x^i(t)\right] + \sum_{j=1}^{N} g_{ij} h\left[x^j(t-\tau)\right]$$

with $x^i \in \mathbb{R}^n$. Here, $g_{ij} \in \mathbb{R}$ is the coupling matrix determining the coupling topology and the strength of each link in the network, f is the (non-linear) function describing the dynamics of an isolated unit, and h is a possibly non-linear coupling function. A synchronized solution can only exist if the row sum of the matrix is the same for each row, i.e., $\sigma = \sum_{j=1}^{N} g_{ij}$ independent of i. In this case if the systems start in a synchronized state $x^1 = x^2 = \cdots = x^N = \overline{x}(t)$, they will remain synchronized since the feedback term will be equal for all x^i. The synchronized solution $\overline{x}(t)$ is then determined by

$$(3.2) \qquad \frac{d}{dt} \overline{x}(t) = f\left[\overline{x}(t)\right] + \sigma h\left[\overline{x}(t-\tau)\right].$$

To calculate the stability of this synchronized solution, we consider the evolution of small perturbations $\xi^i(t)$

$$x^i(t) = \overline{x}(t) + \xi^i(t).$$

Inserting this ansatz into Eq. (3.1) and linearizing in ξ^i we find

$$(3.3) \qquad \frac{d}{dt} \xi^i(t) = Df\left[\overline{x}(t)\right] \xi^i(t) + \sum_{j=1}^{N} g_{ij} Dh\left[\overline{x}(t-\tau)\right] \xi^j(t-\tau),$$

where Df and Dh are Jacobians. Using the vector

$$\Xi(t) = (\xi^1(t),\, \xi^2(t),\ldots,\, \xi^N(t))$$

the system of linear equations (3.3) can be written as

$$(3.4) \qquad \frac{d}{dt} \Xi(t) = I_N \otimes Df\left[\overline{x}(t)\right] \Xi(t) + g \otimes Dh\left[\overline{x}(t-\tau)\right] \Xi(t-\tau),$$

where I_N denotes the N-dimensional identity matrix and $g = (g_{ij})$ is the coupling matrix. We assume that the coupling matrix g is diagonalizable, i.e., there exists a unitary transformation U such that

$$U g U^{-1} = \mathrm{diag}(\sigma,\, \gamma_1,\, \gamma_2,\, \ldots,\, \gamma_{N-1}).$$

Here, σ is the row sum of g, which is always an eigenvalue of g corresponding to the eigenvector $(1, 1, \ldots, 1)$. We call this the *longitudinal* eigenvalue of g. The other eigenvalues γ_k we then call the *transversal* eigenvalues of g.

Diagonalizing g in Eq. (3.4) with the transformation U does not affect the term $I_N \otimes Df[\overline{x}(t)]$ in Eq. (3.4), since this transformation acts only on the matrix I_N. Thus after the diagonalization Eq. (3.4) is transformed into N equations

$$(3.5) \qquad \frac{d}{dt} \xi(t) = Df\left[\overline{x}(t)\right] \xi(t) + \sigma\, Dh\left[\overline{x}(t-\tau)\right] \xi(t-\tau),$$

$$(3.6) \qquad \frac{d}{dt} \xi(t) = Df\left[\overline{x}(t)\right] \xi(t) + \gamma_k\, Dh\left[\overline{x}(t-\tau)\right] \xi(t-\tau)$$

with $k = 1, \ldots, N - 1$. The first equation corresponds to perturbations in the direction of the vector $(1, 1, \ldots, 1)$, which act equally on each individual system and thus do not cause desynchronization. A growing perturbation in this direction indicates that the synchronized solution of the network is chaotic.

The $N - 1$ other equations in (3.6) describe perturbations transversal to the SM. The synchronized solution is stable if and only if these perturbations decay, i. e., if the maximum Lyapunov exponent arising from the variational Eq. (3.6) is negative for all transversal eigenvalues γ_k.

Pecora and Carroll [5] defined a function $\lambda_{\max} : \mathbb{C} \to \mathbb{R}$, which maps a complex number $re^{i\phi}$ to the maximum Lyapunov exponent arising from the variational equation

$$\frac{d}{dt}\xi(t) = Df\left[\overline{x}(t)\right]\xi(t) + re^{i\phi}Dh\left[\overline{x}(t - \tau)\right]\xi(t - \tau).$$

This function is called the master stability function and it can be calculated numerically. Once this function is known on a sufficiently large domain in $\mathbb{C}$, one can immediately decide for any network structure whether synchronization will be stable or not. One only needs to evaluate the MSF at the transversal eigenvalues γ_k of the particular network's coupling matrix. Thus the condition for stable synchronization is then

$$(3.7) \qquad\qquad \lambda_{\max}(\gamma_k) < 0, \quad k = 1, \ldots, N - 1.$$

This way the problem has been separated into one part that only depends on the dynamics of the individual system, and another part that only depends on the coupling topology.

We will now restrict our analysis to maps, but all ingredients of our arguments are also valid for flows and we will point out where the results differ slightly for flows. Delay coupled maps have been widely studied because they show similar behavior as delay differential equation and interesting synchronization phenomena have been found in these systems [55].

For delay coupled maps the dynamics in the SM is governed by the equation

$$(3.8) \qquad\qquad x_{k+1} = f(x_k) + \sigma h(x_{k-\tau})$$

with $\tau \in \mathbb{N}$ and $x_k \in \mathbb{C}^d$ or $\in \mathbb{R}^d$ and the MSF is calculated from

$$(3.9) \qquad\qquad \xi_{k+1} = Df(x_k)\xi_k + re^{i\psi}Dh(x_{k-\tau})\xi_{k-\tau}.$$

Whether the synchronized dynamics is chaotic or not depends on whether the MSF evaluated at the eigenvalue $re^{i\psi} = \sigma$, which corresponds to perturbations parallel to the SM, is positive or not.

With the matrix coefficients $A_k := Df(x_k)$, and $B_k := Dh(x_{k-\tau})$ the variational equation is given by

$$(3.10) \qquad\qquad \xi_{k+1} = A_k\xi_k + re^{i\psi}B_k\xi_{k-\tau}.$$

Note that when the delay is changed the dynamics in the SM changes, too. Hence, we are not able to make predictions about what happens as τ is changed. However, at a fixed large value of the delay time τ we can compare the Lyapunov exponents arising from different values of $re^{i\psi}$ in Eq. (3.9).

We will now analyze the Lyapunov exponents arising from Eq. (3.10) in the limit of large τ. We do this in the following steps: first we analyse the two simpler cases, where the dynamics in the SM is a fixed point (FP) or a periodic orbit (PO). Then

to expand the results to chaotic trajectories x_k in the SM we use the fact that POs are dense in a chaotic attractor.

3.1. **A fixed point in the synchronization manifold.** For FPs of delay differential equations there exists a scaling theory for the FP's eigenvalues in the limit of large delay [56, 57, 58, 59, 60]. Recently this theory has been generalized to the scaling of Floquet exponents [61]. In both cases the eigenvalues or Floquet spectrum consist of two parts: a strongly unstable part arising from unstable eigenvalues of the system without delay and a pseudo-continuous spectrum, for which the real part of the eigenvalues approach zero in the limit of large delay. This scaling theory has been developed for flows. Since we restrict ourselves to maps, we want to discuss the main ideas of the scaling theory for maps now. However, each step can be done in the same way for flows by applying the large delay theory developed in [56, 57, 58, 59, 61].

Let us first consider the case, where the dynamics in the SM is a FP, i.e., a period $T = 1$ orbit. In this case the coefficient matrices in Eq. (3.10) are constant $A = A_k$ and $B = B_k$.

Making the ansatz $\xi_k = z^k \xi_0$, we find an equation for the multipliers z

$$(3.11) \qquad \chi(z) = \det[A - zI + re^{i\psi} B\, z^{-\tau}] = 0,$$

where I denotes the identity matrix.

For the strongly unstable spectrum we suppose there is a solution with $|z| > 1$. Then in the limit of $\tau \to \infty$ Eq. (3.11) becomes

$$(3.12) \qquad \det[A - zI] = 0.$$

Thus in the limit of large delay the eigenvalues z of A with $|z| > 1$ are also solutions of Eq. (3.11).

We are now interested in the pseudo-continuous spectrum, i.e., in the solutions with $|z| \approx 1$ in the limit of large τ. We make the ansatz $z = (1 + \delta/\tau)e^{i\omega}$. In the limit $\tau \to \infty$ we have $(1 + \delta/\tau)^{-\tau} \to e^{-\delta}$, and $(1 + \delta/\tau) \to 1$. Thus in the limit $\tau \to \infty$ Eq. (3.11) becomes

$$(3.13) \qquad 0 = \det[A - Ie^{i\omega} + re^{-\delta}e^{i(\psi-\phi)}B]$$

with $\phi = \omega\tau$. The complex equation (3.13) has three variables ϕ, ω, and δ. Hence, it determines real-valued functions $\delta(\omega)$. As a result, it determines the multipliers $z(\omega)$. Let us show how $\delta(\omega)$ can be calculated. In particular, we will see that $\delta(\omega)$ is independent on the phase ψ of the variational equation.

If B is invertible, we can calculate the eigenvalues $\mu = re^{-\delta}e^{i(\psi-\phi)}$ in the following equation

$$(3.14) \qquad 0 = \det[-B^{-1}(A - Ie^{i\omega}) - \mu],$$

which is a polynomial in μ. This polynomial has exactly d roots μ_j $(j = 1, \ldots, d)$, which are eigenvalues of $-B^{-1}(A - Ie^{i\omega})$. Since Eq. (3.14) is independent of ψ, μ does not depend on ψ as well.

If B is not invertible, Eq. (3.13) still gives a polynomial in μ, for which the roots can be calculated. Then each eigenvalue μ will be a function of ω and one can find the branches

$$\delta(\omega) = \ln\left[\frac{r}{|\mu(\omega)|}\right] = -\ln|\mu(\omega)| + \ln r.$$
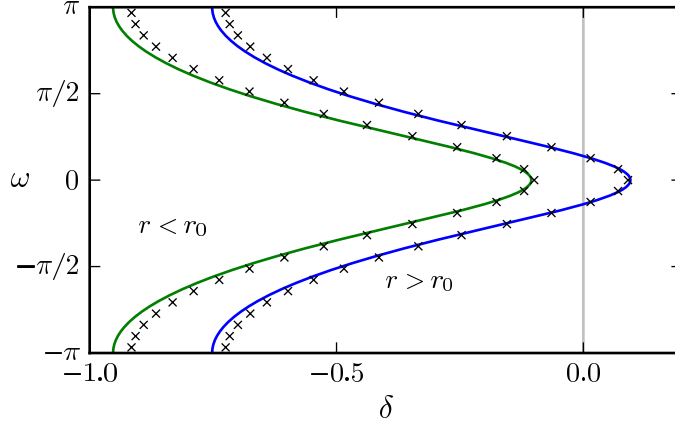
FIGURE 1. Pseudo continuous spectrum $\delta(\omega)$ (lines) and location of the exact roots (crosses) for the example of a one dimensional complex map for $r = 3.3 > r_0 = 3$ and $r = 2.7 < r_0 = 3$. Parameters: $a = 0.4$, $b = 0.2$, $\psi = 0$, $\tau = 30$.

The function $\mu(\omega)$ can admit the zero value at some point ω_0, i.e., $\mu(\omega_0) = 0$, in the case when the matrix A has an eigenvalue with $|z| = 1$. Indeed, as follows from Eq. (3.14), for $\mu = 0$, $\omega = \omega_0$ and $\det B \neq 0$ we have

$$\det[A - Ie^{i\omega_0}] = \det[A - Iz] = 0.$$

In all other cases, with $\det B \neq 0$ and $|z| \neq 1$, the function $|\mu(\omega)|$ is bounded $0 < \mu_0 \leq |\mu(\omega)| \leq \mu_1$.

If there are no strongly unstable eigenvalues, the sign of δ determines the stability in the limit of large τ. It is clear, that δ increases monotonically with increasing r and in particular δ is negative for small r and positive for large r. Thus there is a minimum radius r_0, for which the first eigenvalue branch becomes unstable $\delta > 0$ and thus the MSF changes sign.

Note that we have obtained the function $\delta(\omega)$ on which the solutions lie in the limit of large τ but not yet the exact values of ω. These are not important in the limit of large delay, since the eigenvalues become very dense on the curve $\delta(\omega)$. Indeed, the exact values of ω can be calculated from the expression $\mu(\omega) = re^{-\delta(\omega)}e^{i(\psi - \omega\tau)}$, which implies

(3.15) $$\operatorname{Arg}\mu(\omega) = \psi - \omega\tau + 2\pi k$$

for any integer k. Since $\mu(\omega)$ is a known eigenvalue of the matrix $-B^{-1}(A - Ie^{i\omega})$, Eq. (3.15) can be considered as a transcendental equation for determining the solutions $\omega = \omega_k$. In particular, Eq. (3.15) implies that the distance between the neighboring solutions ω_k and ω_{k-1} reads

$$\omega_k - \omega_{k-1} = \frac{1}{\tau}\left[\operatorname{Arg}\mu(\omega_{k-1}) - \operatorname{Arg}\mu(\omega_k)\right] + \frac{2\pi}{\tau}$$

$$= 2\pi/\tau + \mathcal{O}\left(1/\tau^2\right).$$

Thus it is proportional to $1/\tau$ and the curve $\delta(\omega)$ is filled densely with roots as $\tau \to \infty$.
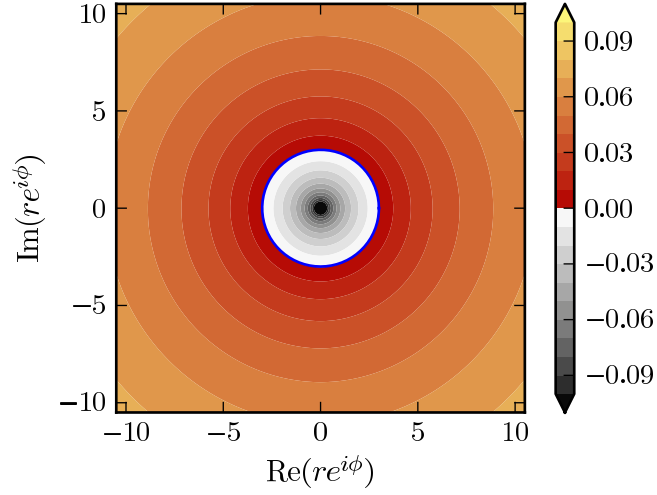
FIGURE 2. Master stability function for a one-dimensional map with fixed point dynamics in the synchronization manifold. The red regions correspond to $\lambda_{\max} > 0$ (synchronized state is unstable). The gray regions correspond to $\lambda_{\max} < 0$ (synchronized state is stable). The blue circle indicates the stability boundary given by r_0 according to Eq. (3.16). Already for relatively low values of τ the blue line matches very well the numerically obtained boundary. Parameters of the variational equation: $a = 0.4$, $b = 0.2$, $\tau = 20$.
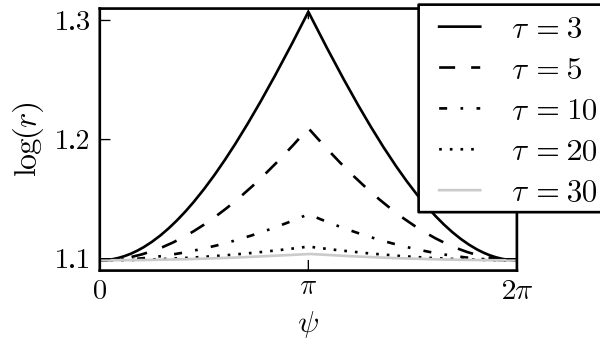

FIGURE 3. Boundary $r(\psi)$ of stability domain in polar coordinates for different values of τ in logarithmic scale. With increasing τ $r(\psi) \to r_0$. Parameters of the variational equation: $a = 0.4$, $b = 0.2$.

Note that the curve $\delta(\omega)$ is determined in the bounded interval $\omega \in [0, 2\pi]$ in contrast to the case of delay differential equations [57], where ω varies on the whole axis $(-\infty, \infty)$.

The simple case is that of a one dimensional ($d = 1$) complex map, where $A = a \in \mathbb{C}$ and $B = b \in \mathbb{C}$ with $|a| < 1$. In this case we can explicitly calculate

$$\delta(\omega) = \ln(|rb|/|a - e^{i\omega}|).$$

For $r < (1 - |a|)/|b|$ all the eigenvalues approach magnitude 1 from the stable side and for $r > (1 - |a|)/|b|$ there are always weakly unstable eigenvalues. Thus the MSF changes sign at

$$(3.16) \qquad\qquad\qquad\qquad r_0 = (1 - |a|)/|b|.$$

The pseudo-continuous spectrum for these two cases is depicted in Fig. 1. The corresponding MSF is shown in Fig. 2. As $\tau \to \infty$, the $\lambda_{\max} = 0$ contour line approaches the circle with radius r_0. This is depicted in Fig. 3, where the angle-dependence of the critical radius is shown for different values of τ in a logarithmic scale. For small values of τ, the critical radius has a strong angle-dependency. However, already for a value of $\tau = 20$, the rotation symmetry is almost perfect (see Fig. 2).

3.2. A periodic orbit in the synchronization manifold. Now consider the map

$$(3.17) \qquad\qquad\qquad\qquad \xi_{k+1} = A_k \, \xi_k + r e^{i\psi} B_k \, \xi_{k-\tau},$$

where A_k and B_k are periodic with period T, corresponding to a PO in the SM. We consider the case of large delay $\tau \gg T$.

Making a Floquet–like ansatz $\xi_k = z^k \, q_k$, where q_k is T periodic we find

$$(3.18) \qquad\qquad\qquad z \, q_{k+1} = A_k \, q_k + r e^{i\psi} B_k \, z^{-\tau} q_{k-n}$$

with $n = \tau \bmod T \in \{0, 1, \dots, T - 1\}$.

For the strongly unstable spectrum again suppose there is a solution with $|z| > 1$, then in the limit $\tau \to \infty$ the term $z^{-\tau}$ vanishes and we find

$$(3.19) \qquad\qquad\qquad\qquad z \, q_{k+1} = A_k \, q_k.$$

Using the periodicity of q_k, Eq. (3.19) implies

$$\det[z^T - \prod_{k=1}^{T} A_k] = 0,$$

where z^T is a Floquet multiplier of the system $\xi_{k+1} = A_k \xi_k$ without delay.

Hence, if z^T is a Floquet multiplier of Eq. (3.19), with $|z| > 1$, then in the limit $\tau \to \infty$ there exists also a solution of Eq. (3.17), which is close to z and vice versa. The rigorous proof of this fact as well as the convergence for the pseudo-continuous spectrum is more tedious and we do not discuss it here. The proof for the case of flows can be found in Ref. [62].

For the pseudo-continuous spectrum we again make the ansatz $z = (1 + \delta/\tau)e^{i\omega}$ and taking the limit $\tau \to \infty$ Eq. (3.18) becomes

$$(3.20) \qquad\qquad\qquad e^{i\omega} \, q_{k+1} = A_k \, q_k + r e^{-\delta} e^{i(\psi - \phi)} B_k \, q_{k-n}$$

with $\phi = \omega\tau$. One thus has to solve

$$(3.21) \qquad\qquad\qquad\qquad 0 = [e^{i\omega}\overline{J} + \overline{A} + \mu\overline{B}]\vec{q} = 0,$$

where $\overline{A} = \mathrm{diag}\{A_1, \ldots, A_T\}$,

$$\overline{J} = \begin{bmatrix} 0 & & & I \\ I & \ddots & & \\ & \ddots & \ddots & \\ & & I & 0 \end{bmatrix}, \quad \overline{B} = \begin{bmatrix} 0 & & & B_1 & & \\ & \ddots & & & \ddots & \\ & & \ddots & & & B_n \\ B_{n+1} & & & \ddots & & \\ & \ddots & & & \ddots & \\ & & B_T & & & 0 \end{bmatrix},$$

$\mu = re^{-\delta}e^{i(\psi-\phi)}$, and $\vec{q} = (q_1, \ldots, q_T)$. The position of the diagonal lines in the matrix $\overline{B}$ depends on the value of $n = \tau \bmod T$. Taking the determinant of the matrix in Eq. (3.21) results in a polynomial in $\mu = re^{-\delta}e^{i(\psi-\phi)}$ (of maximum order $d \times T$). Again, the roots μ are functions of ω and we can calculate the branches $\delta(\omega) = -\ln|\mu(\omega)| + \ln r$, where ψ and ϕ drop out. As in the case of FPs, one can show that the function $|\mu(\omega)|$ is bounded $0 < \mu_0 \leq |\mu(\omega)| \leq \mu_1$ unless the instantaneous system has a Floquet multiplier z with $|z| = 1$.

We have again found the same structure of the MSF : The MSF is rotationally symmetric in the complex plane about the origin. If without feedback ($r = 0$) the MSF is positive, then it is constant in the limit of large delay. Otherwise it is a monotonically increasing function of r and there is a critical radius r_0 where it changes sign.

3.3. A chaotic attractor in the synchronization manifold.

In every chaotic attractor there is an infinite number of unstable periodic orbits (UPOs) embedded. It has been long known that the characteristic properties of the chaotic system can be described in terms of these PO [63]. Intuitively, the chaotic trajectory follows the UPOs closely and "switches" between them, thus averaging over the UPOs in the appropriate way allows us to calculate statistical properties of the attractor. One of the most important examples is the natural measure of the chaotic attractor, which is concentrated at the UPO (hot-spots) and can in fact be expressed in terms of the orbit's Floquet multipliers [64, 65].

Lyapunov exponents arising from variational equations such as Eq. (3.10) have been discussed in the framework of periodic orbit theory [66, 67, 63, 68], too. In particular it has been shown [69] that a chaotic attractor in an invariant manifold loses its transversal stability in a blow-out bifurcation when the transversely unstable orbits outweigh the transversely stable orbits. To be precise, we divide the orbits into two groups of transversely stable and unstable orbits and define [69] the transversely stable weight Λ_T^s and the unstable weight Λ_T^u as

$$(3.22) \qquad \Lambda_T^{u,s} = \sum_{j=1}^{N_T^{u,s}} \mu_T(j)\lambda_T(j),$$

where the sum goes over all N_T^u transversely unstable and N_T^s transversely stable orbits of period T, respectively. Here, $\mu_T(j)$ is the weight of the jth orbit, corresponding to the natural measure of a typical trajectory in the neighborhood of the jth orbit and $\lambda_T(j)$ is the transversal Lyapunov exponent of this jth orbit. The weight of a PO is inversely proportional to the product of its unstable Floquet multipliers [64, 68]. The attractor is transversely unstable if and only if in the limit of large T

$$(3.23) \qquad \Lambda_T^u > |\Lambda_T^s|.$$

TABLE 1.   Stability of chaotic and non-chaotic synchronized solutions for the three types of networks.

	chaotic dynamics in the SM ($r_0 < |\sigma|$)	PO or FP in the SM ($|\sigma| < r_0$)
(A) $|\gamma_{\mathrm{max}}| < |\sigma|$	synchr. stable if $|\gamma_{\mathrm{max}}| < r_0$	synchr. stable
(B) $|\gamma_{\mathrm{max}}| = |\sigma|$	synchr. unstable	synchr. stable
(C) $|\gamma_{\mathrm{max}}| > |\sigma|$	synchr. unstable	synchr. stable if $|\gamma_{\mathrm{max}}| < r_0$

We now make the connection to the scaling theory for large τ. Starting from $r = 0$ (no feedback) transversal Lyapunov exponents $\lambda_T(j)$ of each orbit can only increase with increasing r, as shown above. In particular for large enough r the orbits become transversely unstable: either they are already unstable for $r = 0$ and thus remain unstable or the pseudo-continuous spectrum goes to zero and for large r it does so from the unstable side. Thus there exists a minimum radius r_0, for which the condition (3.23) on the weights is fulfilled. Note that since we consider the limit $\tau \to \infty$ we can evaluate Eq. (3.23) at arbitrarily large T, although it is a common result of PO theory that formulas such as Eq. (3.22) converge quickly.

Thus in summary the MSF has the same structure as for FPs and POs (the rotation symmetry follows from the rotation symmetry of each $\lambda_T(j)$).

4. CONSEQUENCES FOR SYNCHRONIZATION OF NETWORKS

Let us now discuss what the structure of the MSF means for the synchronizability of networks. We can categorize networks into three types depending on the magnitude of the largest transversal eigenvalue γ_{max} in relation to the magnitude of the row sum σ: (A) the largest transversal eigenvalue is strictly smaller than the magnitude of the row sum ($|\gamma_{\mathrm{max}}| < |\sigma|$), (B) the largest transversal eigenvalue has the same magnitude as the row sum ($|\gamma_{\mathrm{max}}| = |\sigma|$), and (C) the largest transversal eigenvalue has a larger magnitude than the row sum ($|\gamma_{\mathrm{max}}| > |\sigma|$).

At $r = |\sigma|$ the MSF is positive ($r_0 < |\sigma|$) for chaotic dynamics in the SM and negative ($|\sigma| < r_0$) for dynamics on a stable PO or a FP. This gives us a lower or an upper bound on r_0 and we can thus give the classification as shown in Table 1. In networks of type (A) and (B) synchronization on a FP or a PO, which is stable within the SM, is always stable. For type (C) this dynamics may be stable or not depending on the particular network (value of $|\gamma_{\mathrm{max}}|$) and the dynamics in the SM (value of r_0). On the other hand chaos synchronization is always unstable in networks of type (B) and (C) and it may be stable or not in networks of type (A) again depending on the particular network and the dynamics.

Note that for autonomous flows with a stable PO in the SM we always have $r_0 = |\sigma|$, due to the PO's Goldstone mode. Thus for this case we cannot decide whether synchronization for type (B) networks will be stable or not. This depends on whether the $\lambda_{\mathrm{max}} = 0$ contour line of the MSF approaches the circle with radius
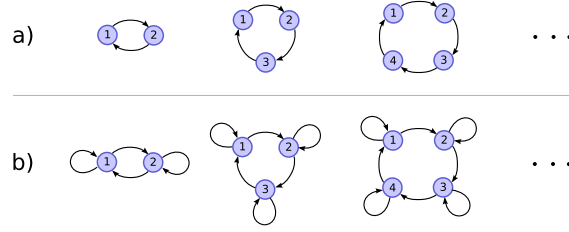
FIGURE 4. (a) unidirectionally coupled rings without feedback: always class (B) (no chaos synchronization), (b) unidirectionally coupled rings with feedback (for positive coupling): class (A) (chaos synchronization possible).

$r_0 = |\sigma|$, locally, at the transversal eigenvalues with $|\gamma_k| = |\sigma|$, from the outside (stable) or from the inside (unstable).

We now list some examples for the three types of networks (Fig. 4). The categorization follows from the eigenvalue structure (spectral radius) for the corresponding matrices, which can, for instance, be derived using Gerschgorin's theorem.

- Mean field coupled systems (all-to-all coupling) have $\gamma_k = 0$ for all k and are thus of type (A).
- Networks with only inhibitory connections (negative entries) or only excitatory connections (positive entries) are up to the row sum factor stochastic matrices, i. e., the coupling matrix G can be written as

$$G = \sigma P ,$$

  where P is a stochastic matrix (non-negative entries and unity row sum). For stochastic matrices it is well known that the spectral radius is one, i. e., all eigenvalues have magnitude smaller than or equal to one. The proof utilizes Gerschgorin's theorem [70]. Thus it follows for G that no eigenvalues has magnitude larger than $|\sigma|$ and these networks are of type (A) or (B).
- Any network with zero row sum ($\sigma = 0$) is of type (B) (trivial case) or (C).
- Rings of uni-directionally coupled elements and two bidirectionally coupled elements are of type (B) [36].
- Unidirectionally coupled rings with self-feedback are for positive couplings of type (A).
- Bidirectionally coupled rings with even number of elements without self-feedback are of type (B).
- Bidirectionally coupled rings with odd number of elements are of type (A).

In the literature there is a great amount of material on the relation of the spectral radius and the row sum for certain types of matrices. These results are immediately applicable to our classification. For a concrete network topology the classification is of course very simple.

Networks with $\sigma = 0$ belong to class (B) (trivial case) or to class (C). This confirms the conjecture stated in [35]: Networks for which the trajectory of an uncoupled unit is also a solution of the network ($\sigma = 0$) cannot exhibit chaos synchronization for large coupling delay.
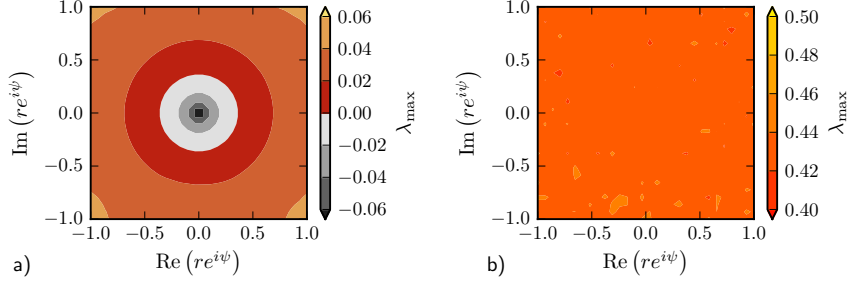
FIGURE 5.   Master stability function (shown in color) for delay coupled logistic maps (Eq. (4.2)). Panel (a) corresponds to $\lambda = 3.2$ and the stable period-2 orbit within the SM. Panel (b) corresponds to $\lambda = 3.8$ and a chaotic attractor within the SM. In both cases the delay is chosen as $\tau = 30$.

For the chaotic case there may exist another radius r_b, with $0 \leq r_b \leq r_0$, where the first PO in the attractor loses its transverse stability and the attractor undergoes a bubbling bifurcation [26, 71, 42]. Then any network with $r_b < |\gamma_{\max}| < r_0$ will exhibit bubbling in the presence of noise (or parameter mismatch), while any network with $|\gamma_{\max}| < r_b$ will show stable synchronization, even in the presence of noise.

In order to illustrate the obtained results, let us consider the following example of linearly coupled logistic maps

$$(4.1) \qquad x_{k+1}^m = \lambda x_k^m (1 - x_k^m) + \sum_{j=1}^{N} g_{mj} x_{k-\tau}^j$$

with the zero row sums $\sigma = 0$. The MSF is calculated from the following delayed system

$$(4.2) \qquad \xi_{k+1} = \lambda(1 - 2x_k)\xi_k + re^{i\psi}\xi_{k-\tau},$$

where the dynamics on the synchronization manifold x_k is determined by the map $x_{k+1} = \lambda x_k (1 - x_k)$. Figure 5 shows numerically computed MSF, i.e., the largest Lyapunov exponent of the system (4.2) for two different cases: $\lambda = 3.2$ and $\lambda = 3.8$, which correspond to the stable period-2 state and chaos, respectively. The delay is set to $\tau = 30$. In both cases, the MSF are radially symmetric. In the stable periodic case (panel (a)), there exists a critical radius r_0 where the MSF changes sign, which determines the synchronizability of a given coupled system. In the chaotic case (panel (b)) the MSF is close to a positive constant, i.e., any coupling configuration will be unstable.

For the parameters used in panel (b) the dynamics exhibits so-called *strong chaos* [72]. Strong chaos is characterized by a Lyapunov exponent that stays constant with increasing delay time. As recently shown [72] chaos synchronization is not possible in the large delay limit for strong chaos. The other case of *weak chaos* occurs when the largest Lyapunov exponent scales as $1/\tau$ for $\tau \to \infty$. In this case chaos synchronization is possible and the critical radius is determined by

$$(4.3) \qquad r_0 = |\sigma|e^{-\lambda_m \tau},$$

where λ_m is the maximum Lyapunov exponent of the system [72].

5. Experimental setup for finding the critical radius

We now propose an experimental method for determining the critical radius r_0. Consider two elements coupled in the following network motif

$$x_{k+1}^1 = f(x_k^1) + \mu h(x_{k-\tau}^1) + \nu h(x_{k-\tau}^2),$$
$$x_{k+1}^2 = f(x_k^2) + \mu h(x_{k-\tau}^2) + \nu h(x_{k-\tau}^1),$$

where μ and ν are the self feedback strengths and the coupling strengths, respectively. Suppose we are able to change the self-feedback strengths μ and the coupling strengths ν, for example by using gray filters in an optical experiment.

Let us choose

$$\mu = \tfrac{1}{2}(\sigma + r) \qquad \text{and} \qquad \nu = \tfrac{1}{2}(\sigma - r).$$

Then the dynamics in the SM is given by

$$x_{k+1} = f(x_k) + \sigma h(x_{k-\tau}),$$

while the variational equation transverse to the SM is given by

$$\xi_{k+1} = Df(x_k)\xi_k + rDh(x_{k-\tau})\xi_{k-\tau}.$$

Thus by changing r (for fixed σ) and checking whether the two elements synchronize we are able to probe the MSF along the real axis at the radius r. Due to the monotonicity we can use a root-finding algorithm such as the bisection method to find r_0 to high accuracy with little iterations of the experiment and without knowledge of the functions f and h. We can repeat this procedure for other values of σ and obtain the critical radius as a function of $r_0(\sigma)$. Thus from this rather simple setup we can decide for any network of these elements whether synchronization is stable or not.

As an example we consider two optoelectronically coupled lasers

$$\frac{d}{dt}\rho_1 = n_1\rho_1,$$

(5.1a) $$T\frac{d}{dt}n_1 = p + \mu\rho_1(t-\tau) + \nu\rho_2(t-\tau) - n_1 - (1+n_1)\rho_1,$$

$$\frac{d}{dt}\rho_2 = n_2\rho_2,$$

(5.1b) $$T\frac{d}{dt}n_2 = p + \mu\rho_2(t-\tau) + \nu\rho_1(t-\tau) - n_2 - (1+n_2)\rho_2,$$

where ρ_i and n_i is the intensity and the carrier density of the ith laser, respectively. The pump current of each laser is modulated by the delayed intensities according to the coupling scheme depicted in Fig. 6. Such feedback can be realized by using photodiodes to measure the intensities of the arriving signals and modulating the pump current accordingly. The bidirectional coupling has strength ν and the self-feedback of each laser has strength μ. For this setup we have numerically calculated $r_0(\sigma)$ in the same manner as it would be done in an experiment: We choose a value of σ, an interval $I_r = [r_{\min}, r_{\max}]$ for the r-domain and an initial value of $r = r_0$. We consider the systems to be synchronized, if the relative synchronization error

$$\varepsilon := \frac{\langle|\rho_1 - \rho_2|\rangle}{\frac{1}{2}[\langle\rho_1\rangle + \langle\rho_2\rangle]}$$
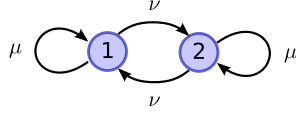
FIGURE 6. Schematic setup for determining the critical radius in an experiment.
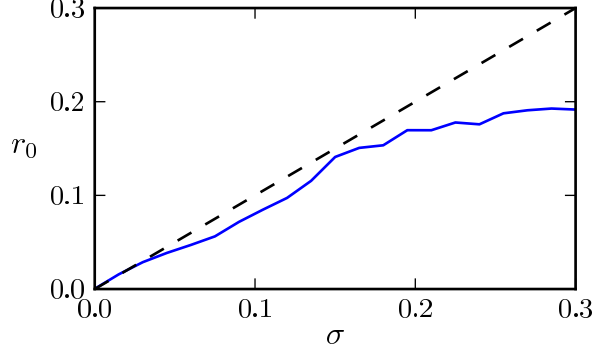

FIGURE 7. Numerically calculated critical radius r_0 as a function of σ (solid curve) for the system of optoelectronically coupled lasers corresponding to Eqs. (5.1). A network can only have a stable synchronized solution if the magnitudes of its transversal eigenvalues are below the curve. The curve is calculated up to an absolute error of 10^{-4}. The dashed line shows the diagonal line $r_0 = \sigma$. Parameters: $\varepsilon_0 = 10^{-7}$, $p = 1$, $T = 200$, $\tau = 2000$.

is smaller than a threshold ε_0. We then simulate the system and use the bisection method to find the synchronization threshold r_0 (up to a desired accuracy) in the interval I_r. We can then use the calculated value of r_0 as an initial guess for neighboring σ-values and thus follow the curve $r_0(\sigma)$.

The result is depicted in Fig. 7, where the solid curve shows $r_0(\sigma)$ and the dashed line corresponds to $r_0 = \sigma$. For small values of σ, i. e., weak feedback, the dynamics is a PO and due to the Goldstone mode we have $r_0 \approx \sigma$. For larger values of σ, the system becomes chaotic and $r_0 < \sigma$. For a given value of σ, a network has a stable synchronized solution if and only if all transversal eigenvalues γ_k of the corresponding coupling matrix have magnitude $|\gamma_k| < r_0(\sigma)$.

A similar method has been implemented in [73]. Here the structure of the MSF was confirmed experimentally using optoelectronic oscillators.

6. CONCLUSION AND OUTLOOK

In conclusion we have shown that the MSF has a simple structure in the limit of large delay: it is rotationally symmetric around the origin and either positive and constant (if it is positive at the origin) or monotonically increasing and becomes positive at a minimum radius r_0. This structure allowed us to prove a recent conjecture [35] about synchronizability of chaotic elements. Furthermore, we classified network structures into three types depending on the magnitude of the maximum

transversal eigenvalue in relation to the magnitude of the row sum and showed that these network types have distinct synchronization properties. Using several prototype networks like all-to-all or ring topologies we illustrated the scope of these three classes. By means of a motif of two coupled nodes with feedback loops, we proposed a very simple scheme with which the critical radius r_0 can be found experimentally. Instead of mapping out the entire domain of the master stability function, the knowledge of the rotational symmetry allows the two-node motif to predict stability of any network using the same local dynamics in the case of large delay times.

The rotational symmetry of the MSF has previously been found numerically [36, 52]. In Ref. [52] the same structure of the MSF has been found for a PO in the SM for which the period T is approximately equal to the delay time τ. For this case the structure of the MSF has also been derived analytically in [52]. Note that this case is complementary to the situation $T \ll \tau$ that we looked at in this paper. So the structure of the MSF that we found seems to be valid in even more general cases.

References

[1] A. S. Pikovsky, M. G. Rosenblum, and J. Kurths: *Synchronization, A Universal Concept in Nonlinear Sciences* (Cambridge University Press, Cambridge, 2001).

[2] S. Boccaletti, J. Kurths, G. Osipov, D. L. Valladares, and C. S. Zhou: *The synchronization of chaotic systems*, Phys. Rep. **366**, 1 (2002).

[3] E. Mosekilde, Y. Maistrenko, and D. Postnov: *Chaotic Synchronization: Applications to Living Systems* (World Scientific, Singapore, 2002).

[4] A. G. Balanov, N. B. Janson, D. E. Postnov, and O. V. Sosnovtseva: *Synchronization: From Simple to Complex* (Springer, Berlin, 2009).

[5] L. M. Pecora and T. L. Carroll: *Synchronization in chaotic systems*, Phys. Rev. Lett. **64**, 821 (1990).

[6] C. U. Choe, V. Flunkert, P. Hövel, H. Benner, and E. Schöll: *Conversion of stability in systems close to a Hopf bifurcation by time-delayed coupling*, Phys. Rev. E **75**, 046206 (2007).

[7] E. Schöll and H. G. Schuster (Eds.): *Handbook of Chaos Control* (Wiley-VCH, Weinheim, 2008), second completely revised and enlarged edition.

[8] W. Just, A. Pelster, M. Schanz, and E. Schöll (Eds.): *Delayed complex systems*, Theme Issue of Phil. Trans. R. Soc. A **368** (2010), pp.301-513.

[9] F. M. Atay (Ed.): *Complex Time-Delay Systems*, Understanding Complex Systems (Springer, Berlin Heidelberg, 2010).

[10] I. Fischer, Y. Liu, and P. Davis: *Synchronization of chaotic semiconductor laser dynamics on subnanosecond time scales and its potential for chaos communication*, Phys. Rev. A **62**, 011801 (2000).

[11] T. Heil, J. Mulet, I. Fischer, C. R. Mirasso, M. Peil, P. Colet, and W. Elsäßer: *On/off phase shift keying for chaos-encrypted communication using external-cavity semiconductor lasers*, IEEE J. Quantum Electron. **38**, 1162 (2002).

[12] A. Argyris, D. Syvridis, L. Larger, V. Annovazzi-Lodi, P. Colet, I. Fischer, J. García-Ojalvo, C. R. Mirasso, L. Pesquera, and K. A. Shore: *Chaos-based communications at high bit rates using commercial fibre-optic links*, Nature **438**, 343 (2005).

[13] D. M. Kane and K. A. Shore (Editors): *Unlocking Dynamical Diversity: Optical Feedback Effects on Semiconductor Lasers* (Wiley VCH, Weinheim, 2005).

[14] W. Kinzel and I. Kanter: *Secure communication with chaos synchronization*, in *Handbook of Chaos Control*, edited by E. Schöll and H. G. Schuster (Wiley-VCH, Weinheim, 2008), second completely revised and enlarged edition.

[15] R. Vicente, C. R. Mirasso, and I. Fischer: *Simultaneous bidirectional message transmission in a chaos-bases communication scheme*, Opt. Lett. **32**, 403 (2007).

[16] I. Kanter, E. Kopelowitz, and W. Kinzel: *Public channel cryptography: chaos synchronization and Hilbert's tenth problem*, Phys. Rev. Lett. **101**, 84102 (2008).

[17] I. Kanter, Y. Aviad, I. Reidler, E. Cohen, and M. Rosenbluh: *An optical ultrafast random bit generator*, Nat. Photon. **4**, 58 (2009).

[18] W. Kinzel, A. Englert, and I. Kanter: *On chaos synchronization and secure communication*, Phil. Trans. R. Soc. A **368**, 379 (2010).

[19] A. Englert, W. Kinzel, Y. Aviad, M. Butkovski, I. Reidler, M. Zigzag, I. Kanter, and M. Rosenbluh: *Zero lag synchronization of chaotic systems with time delayed couplings*, Phys. Rev. Lett. **104**, 114102 (2010).

[20] J. Mulet, C. R. Mirasso, T. Heil, and I. Fischer: *Synchronization scenario of two distant mutually coupled semiconductor lasers*, J. Opt. B **6**, 97 (2004).

[21] I. Fischer, R. Vicente, J. M. Buldú, M. Peil, C. R. Mirasso, M. C. Torrent, and J. García-Ojalvo: *Zero-lag long-range synchronization via dynamical relaying*, Phys. Rev. Lett. **97**, 123902 (2006).

[22] E. Klein, N. Gross, M. Rosenbluh, W. Kinzel, L. Khaykovich, and I. Kanter: *Stable isochronal synchronization of mutually coupled chaotic lasers*, Phys. Rev. E **73**, 066214 (2006).

[23] L. B. Shaw, I. B. Schwartz, E. A. Rogers, and R. Roy: *Synchronization and time shifts of dynamical patterns for mutually delay-coupled fiber ring lasers*, Chaos **16**, 015111 (2006).

[24] A. S. Landsman and I. B. Schwartz: *Complete chaotic synchronization in mutually coupled time-delay systems*, Phys. Rev. E **75**, 026201 (2007).

[25] P. Ashwin, J. Buescu, and I. Stewart: *Bubbling of attractors and synchronisation of chaotic oscillators*, Phys. Lett. A **193**, 126 (1994).

[26] E. Ott and J. C. Sommerer: *Blowout bifurcations: the occurrence of riddled basins and on-off intermittency*, Phys. Lett. A **188**, 39 (1994).

[27] M. Sauer and F. Kaiser: *On-off intermittency and bubbling in the synchronization break-down of coupled lasers*, Phys. Lett. A **243**, 38 (1998).

[28] J. R. Terry, K. S. Thornburg, D. J. DeShazer, G. D. VanWiggeren, S. Zhu, P. Ashwin, and R. Roy: *Synchronization of chaos in an array of three lasers*, Phys. Rev. E **59**, 4036 (1999).

[29] D. J. Gauthier and J. C. Bienfang: *Intermittent loss of synchronization in coupled chaotic oscillators: Toward a new criterion for high-quality synchronization*, Phys. Rev. Lett. **77**, 1751 (1996).

[30] V. Flunkert, S. Yanchuk, T. Dahms, and E. Schöll: *Synchronizing distant nodes: a universal classification of networks*, Phys. Rev. Lett. **105**, 254101 (2010).

[31] V. Flunkert: *Delay-Coupled Complex Systems*, Springer Theses (Springer, Heidelberg, 2011).

[32] L. M. Pecora and T. L. Carroll: *Master stability functions for synchronized coupled systems*, Phys. Rev. Lett. **80**, 2109 (1998).

[33] L. M. Pecora and M. Barahona: *Synchronization of Oscillators in Complex Networks*, in *New Research on Chaos and Complexity*, edited by F. F. Orsucci and N. Sala (Nova Science Publishers, 2006), chap. 5, pp. 65–96.

[34] M. Dhamala, V. K. Jirsa, and M. Ding: *Enhancement of neural synchrony by time delay*, Phys. Rev. Lett. **92**, 074104 (2004).

[35] W. Kinzel, A. Englert, G. Reents, M. Zigzag, and I. Kanter: *Synchronization of networks of chaotic units with time-delayed couplings*, Phys. Rev. E **79**, 056207 (2009).

[36] C. U. Choe, T. Dahms, P. Hövel, and E. Schöll: *Controlling synchrony by delay coupling in networks: from in-phase to splay and cluster states*, Phys. Rev. E **81**, 025205(R) (2010).

[37] H. Erzgräber, B. Krauskopf, and D. Lenstra: *Compound laser modes of mutually delay-coupled lasers*, SIAM J. Appl. Dyn. Syst. **5**, 30 (2006).

[38] T. W. Carr, I. B. Schwartz, M. Y. Kim, and R. Roy: *Delayed-mutual coupling dynamics of lasers: scaling laws and resonances*, SIAM J. Appl. Dyn. Syst. **5**, 699 (2006).

[39] O. D'Huys, R. Vicente, T. Erneux, J. Danckaert, and I. Fischer: *Synchronization properties of network motifs: Influence of coupling delay and symmetry*, Chaos **18**, 037116 (2008).

[40] R. Vicente, L. L. Gollo, C. R. Mirasso, I. Fischer, and P. Gordon: *Dynamical relaying can yield zero time lag neuronal synchrony despite long conduction delays*, Proc. Natl. Acad. Sci. **105**, 17157 (2008).

[41] H. J. Wünsche, S. Bauer, J. Kreissl, O. Ushakov, N. Korneyev, F. Henneberger, E. Wille, H. Erzgräber, M. Peil, W. Elsäßer, and I. Fischer: *Synchronization of delay-coupled oscillators: A study of semiconductor lasers*, Phys. Rev. Lett. **94**, 163901 (2005).

[42] V. Flunkert, O. D'Huys, J. Danckaert, I. Fischer, and E. Schöll: *Bubbling in delay-coupled lasers*, Phys. Rev. E **79**, 065201 (R) (2009).

[43] K. Hicke, O. D'Huys, V. Flunkert, E. Schöll, J. Danckaert, and I. Fischer: *Mismatch and synchronization: Influence of asymmetries in systems of two delay-coupled lasers*, Phys. Rev. E **83**, 056211 (2011).

[44] K. Lüdge (Ed.): *Nonlinear Laser Dynamics - From Quantum Dots to Cryptography* (WILEY-VCH, Weinheim, 2011).

[45] E. Rossoni, Y. Chen, M. Ding, and J. Feng: *Stability of synchronous oscillations in a system of Hodgkin-Huxley neurons with delayed diffusive and pulsed coupling*, Phys. Rev. E **71**, 061904 (2005).

[46] C. Hauptmann, O. Omel'chenko, O. V. Popovych, Y. Maistrenko, and P. A. Tass: *Control of spatially patterned synchrony with multisite delayed feedback*, Phys. Rev. E **76**, 066209 (2007).

[47] C. Masoller, M. C. Torrent, and J. García-Ojalvo: *Interplay of subthreshold activity, time-delayed feedback, and noise on neuronal firing patterns*, Phys. Rev. E **78**, 041907 (2008).

[48] E. Schöll, G. Hiller, P. Hövel, and M. A. Dahlem: *Time-delayed feedback in neurosystems*, Phil. Trans. R. Soc. A **367**, 1079 (2009).

[49] M. A. Dahlem, G. Hiller, A. Panchuk, and E. Schöll: *Dynamics of delay-coupled excitable neural systems*, Int. J. Bifur. Chaos **19**, 745 (2009).

[50] P. Hövel, M. A. Dahlem, and E. Schöll: *Control of synchronization in coupled neural systems by time-delayed feedback*, Int. J. Bifur. Chaos **20**, 813 (2010).

[51] S. A. Brandstetter, M. A. Dahlem, and E. Schöll: *Interplay of time-delayed feedback control and temporally correlated noise in excitable systems*, Phil. Trans. R. Soc. A **368**, 391 (2010).

[52] J. Lehnert, T. Dahms, P. Hövel, and E. Schöll: *Loss of synchronization in complex neural networks with delay*, Europhys. Lett. (2011), in print (arXiv:1107.4195).

[53] P. Hövel, M. A. Dahlem, T. Dahms, G. Hiller, and E. Schöll: *Time-delayed feedback control of delay-coupled neurosystems and lasers*, in *Preprints of the Second IFAC meeting related to analysis and control of chaotic systems (CHAOS09)* (World Scientific, 2009), (arXiv:0912.3395).

[54] A. Takamatsu, R. Tanaka, H. Yamada, T. Nakagaki, T. Fujii, and I. Endo: *Spatiotemporal symmetry in rings of coupled biological oscillators of physarum plasmodial slime mold*, Phys. Rev. Lett. **87**, 078102 (2001).

[55] F. M. Atay, J. Jost, and A. Wende: *Delays, connection topology, and synchronization of coupled chaotic maps*, Phys. Rev. Lett. **92**, 144101 (2004).

[56] G. Giacomelli and A. Politi: *Relationship between delayed and spatially extended dynamical systems*, Phys. Rev. Lett. **76**, 2686 (1996).

[57] S. Yanchuk and M. Wolfrum: *Instabilities of equilibria of delay-differential equations with large delay*, in *Proc. 5th EUROMECH Nonlinear Dynamics Conference ENOC-2005, Eindhoven*, edited by D. H. van Campen, M. D. Lazurko, and W. P. J. M. van den Oever (Eindhoven University of Technology, Eindhoven, Netherlands, 2005), pp. 1060–1065, eNOC Eindhoven (CD ROM), ISBN 90 386 2667 3.

[58] S. Yanchuk, M. Wolfrum, P. Hövel, and E. Schöll: *Control of unstable steady states by long delay feedback*, Phys. Rev. E **74**, 026201 (2006).

[59] M. Wolfrum and S. Yanchuk: *Eckhaus instability in systems with large delay*, Phys. Rev. Lett. **96**, 220201 (2006).

[60] M. Lichtner, M. Wolfrum, and S. Yanchuk: *The spectrum of delay differential equations with large delay*, SIAM J. Math. Anal. **43**, 788 (2011).

[61] S. Yanchuk and P. Perlikowski: *Delay and periodicity*, Phys. Rev. E **79**, 046221 (2009).

[62] J. Sieber, M. Wolfrum, M. Lichtner, and S. Yanchuk: *On the stability of periodic orbits in delay equations with large delay*, ArXiv e-prints (2011), arXiv:1101.1197.

[63] P. Cvitanović, R. Artuso, R. Mainieri, G. Tanner, and G. Vattay: *Chaos: Classical and Quantum* (Niels Bohr Institute, Copenhagen, 2008), http://ChaosBook.org.

[64] C. Grebogi, E. Ott, and J. A. Yorke: *Unstable periodic orbits and the dimensions of multifractal chaotic attractors*, Phys. Rev. A **37**, 1711 (1988).

[65] Y. C. Lai, Y. Nagai, and C. Grebogi: *Characterization of the natural measure by unstable periodic orbits in chaotic attractors*, Phys. Rev. Lett. **79**, 649 (1997).

[66] P. Cvitanović and G. Vattay: *Entire Fredholm determinants for evaluation of semiclassical and thermodynamical spectra*, Phys. Rev. Lett. **71**, 4138 (1993).

[67] P. Cvitanović: *Dynamical averaging in terms of periodic orbits*, Physica D **83**, 109 (1995).

[68] M. A. Zaks and D. S. Goldobin: *Comment on "time-averaged properties of unstable periodic orbits and chaotic orbits in ordinary differential equation systems"*, Phys. Rev. E **81**, 018201 (2010).

[69] Y. Nagai and Y. C. Lai: *Periodic-orbit theory of the blowout bifurcation*, Phys. Rev. E **56**, 4031 (1997).

[70] J. Lehnert: *Dynamics of Neural Networks with Delay*, Master's thesis, Technische Universität Berlin (2010).

[71] P. Ashwin, J. Buescu, and I. Stewart: *From attractor to chaotic saddle: a tale of transverse instability*, Nonlinearity **9**, 703 (1996).

[72] S. Heiligenthal, T. Dahms, S. Yanchuk, T. Jüngling, V. Flunkert, I. Kanter, E. Schöll, and W. Kinzel, Phys. Rev. Lett. **107**, 234102 (2011)

[73] L. Illing, C. D. Panda, and L. Shareshian: *Isochronal chaos synchronization of delay-coupled optoelectronic oscillators*, Phys. Rev. E **84**, 016213 (2011).

Institut für Theoretische Physik, TU Berlin, Hardenbergstrasse 36, 10623 Berlin, Germany

Instituto de Fisica Interdisciplinar y Sistemas Complejos,, IFISC (UIB-CSIC), Campus Universitat de les Illes Balears, E-07122 Palma de Mallorca, Spain
   E-mail address: `flunkert@itp.tu-berlin.de`

Institut für Mathematik, Humboldt Universität Berlin, Unter den Linden 6, 10099 Berlin, Germany

Institut für Theoretische Physik, TU Berlin, Hardenbergstrasse 36, 10623 Berlin, Germany

Institut für Theoretische Physik, TU Berlin, Hardenbergstrasse 36, 10623 Berlin, Germany